Journal of Physics: Conference Series **1435** (2020) 012066 doi:10.1088/1742-6596/1435/1/012066

Stability and deformation behavior of three-dimensional diamond-like carbon phases under compression

L. Kh. Rysaeva

Institute for Metals Superplasticity Problems of RAS, 450001, St. Khalturina 39, Ufa, Russia

E-mail: lesya813rys@gmail.com

Abstract. Diamond-like phases which are three-dimensional carbon nanostructures consist of sp^3-hybridized atoms is of high interest in terms of their mechanical properties. The important issues are the stability of such novel structures and their deformation behavior under various conditions. In the present work, the molecular dynamics method is used to study diamond-like phases of two classes: fulleranes and tubulanes. Twelve stable structures are found Studying the deformation behavior shows that some phases have a very small elastic regime which not allow calculating elastic constants. Under hydrostatic compression, the main deformation mechanisms are changing the lattice parameters and valent angles. At high pressure, transformation to the amorphous phase takes place for several diamond-like phases.

1. Introduction

Diamond is one of the well-known carbon allotropes, which is widely used in various practical applications. In addition to diamond, with the development of chemistry and methods of synthesis of modern carbon structures with new properties [1, 2, 3, 4, 5, 6, 7, 8, 9], diamond-like phases of different morphology were also proposed [10, 11, 12, 13, 14, 15]. Diamond-like carbon itself has a non-uniform composition and comes as a mixture of amorphous and crystalline phases [16, 17, 18]. Comparatively, diamond-like carbon phases (DLPs) are totally crystalline phases containing sp^3-coordinated carbon atoms [19, 20, 21, 22, 23]. Three classes of DLPs were proposed: based on fullerene-like molecules - named fulleranes; based on nanotubes - named tubulanes; and based on graphene sheets combined to the 3D structure. It was shown, that DLPs can have hardness close to that of the diamond which means that they can be used as protective coatings. Much more interesting that several DLPs are auxetic materials and have negative Poisson's ratio and quite high Young's modulus [4, 24, 25, 26, 27]. To date, such structures can be hardly obtained experimentally, however, the samples containing both lonsdaleite and diamond phases were obtained in a laboratory environment under conditions of high pressures, and high temperatures [14].

In the present paper, stability and deformation behavior of DLPs based on fullerene-like molecules (fulleranes) and nanotubes (tubulanes) by means of molecular dynamics simulation are studied. Basic mechanisms of non-elastic deformation under hydrostatic compression of such phases are found.

2. Simulation details

The study is carried out using the molecular dynamics (MD) method in freely distributed modeling package LAMMPS, where the interaction of atoms is described by the AIREBO interatomic potential. Simulation cells are created by a home-made program for combining unit cells into a three-dimensional structure of any size. Fig. 1 shows 3D examples of studied stable DLP configurations in perspective view. All the structural parameters can be found in previous works [20, 28, 21, 25, 29, 24]. Ten fulleranes were proposed - CA1, CA2, CA3, CA4, CA5, CA6, CA7, CA8, CA9 and CB; ten tubulanes - TA1, TA2, TA3, TA4, TA5, TA6, TA7, TA8, TA9 and TB. Among them to cubic anisotropy are related eight phases (CA1, CA3, CA4, CA6, CA7, CA8, CA9, CB), to hexagonal - five (CA2, TA2, TA4, TA7, TB), to tetragonal - five (CA3, TA1, TA3, TA5, TA6) and one is trigonal - TA8.

All studies are performed at two temperatures 1 K and 300 K with the use of a Nose-Hoover thermostat. At the initial moment, the structure of the DLP relaxed until it reached a state with minimal potential energy. After that, the calculation of compliance s_{ij} and stiffness c_{ij} moduli is carried out from the Hooke's law [25, 29, 24]. Calculated compliance and stiffness constants are presented in Tab.1 for 14 stable phases. Such elastic constants as Poisson's ratio, Young's modulus, bulk, and shear modulus can be obtained from compliance and stiffness coefficients [30, 31, 32, 33]

To study the mechanical properties, stable configurations are selected based on three criteria: relaxation stability, deformation stability, and thermodynamic (Born) criteria. After applying these three criteria six stable fulleranes (CA2, CA3, CA7, CA8, CA9, CB) from ten proposed phases and six stable tubulanes (TA1, TA3, TA5, TA6, TA8, TB) from nine proposed phases are found.

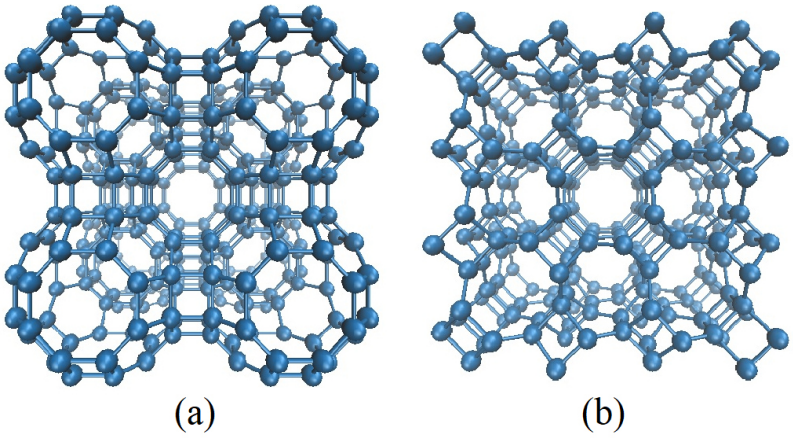

Figure 1. Examples on stable DLPs: (a) fullerane CA7 and (b) tubulane TA5.

To study mechanical properties, hydrostatic compression $\varepsilon_{xx} = \varepsilon_{yy} = \varepsilon_{zz} = \varepsilon$, is applied to the computational cells at the temperature close to 0 K or at 300 K with the strain rate $\dot{\varepsilon} = 0.01\ ps^{-1}$. To characterize the response of DLPs to strain-controlled hydrostatic compression, the corresponding hydrostatic pressure $p = (\sigma_{xx} + \sigma_{yy} + \sigma_{zz})/3$, energies and other characteristics are calculated during the simulation.

For clarity, here results only for fullerane CA7 and tubulane TA5 are presented.

Table 1. Compliance s_{ij} and stiffness c_{ij} coefficients for stable fulleranes and tubulanes.

DLP	s_{11}, TPa^{-1}	s_{12}, TPa^{-1}	s_{13}, TPa^{-1}	s_{33}, TPa^{-1}	s_{44}, TPa^{-1}	s_{66}, TPa^{-1}
CA2	2.515	0.0906	−1.362	1.92	18.4	-
CA3	1.87	−0.44	-	-	2.496	-
CA4	1.87	−0.437	-	-	9.637	-
CA6	1.48	−0.072	-	-	8.66	-
CA7	8.12	−3.82	-	-	3.64	-
CA8	1.67	−0.299	-	-	5.91	-
CA9	3.73	−0.90	-	-	7.31	-
CB	5.53	−2.0	-	-	10	-
TA1	2.15	−0.88	−0.52	2.3	7.90	5.51
TA3	1.9	−0.71	−0.52	2.58	7.76	4.96
TA5	1.55	−0.49	−0.30	1.14	5.60	2.16
TA6	1.47	−0.01	−0.13	0.82	4.73	2.77
TA8	1.98	−0.94	−0.06	0.96	3.88	5.29
TB	1.656	−0.159	−0.29	0.999	10.174	-
DLP	c_{11}, GPa	c_{12}, GPa	c_{13}, GPa	c_{33}, GPa	c_{44}, GPa	c_{66}, GPa
CA2	413	−1.63	87.3	555	161	-
CA3	625	192	-	-	401	-
CA4	624	190			104	-
CA6	1068	87.8	-	-	116	-
CA7	455	370	-	-	262	-
CA8	650	142	-	-	169	-
CA9	316	101	-	-	137	-
CB	306	174	-	-	99.9	-
TA1	652	318	196	461	130	182
TA3	706	294	165	463	129	201
TA5	820	350	226	989	179	463
TA6	1854	55	−8.59	1214	442	221
TA8	657	315	67	1051	188	257
TB	600	−30.5	155	1067	3614	-

3. Results and discussion

In Figs. 2 and 3 the analysis of deformation behavior is presented for fullerane CA7 and tubulane TA5 correspondingly: (a) pressure-strain curves under hydrostatic compression; (b) structural element with main lattice parameters and valent angles; (c,d) changes of the structural characteristics - covalent bonds (c) and valent angles (d).

3.1. Fulleranes

Fig. 2a shows hydrostatic pressure as the function of strain for fullerane CA7 for two temperatures. It can be seen, that the deformation proceeds evenly; temperature does not considerably affect the deformation process. Critical strain value is $\varepsilon = \sim 0.09$ and critical stress is $p = 61$ GPa [29] at 0 K. Relaxation took place during 1 ps (Fig. 2c,d) and elastic range is about 1 % (Fig. 2a).

Considerable changes of all values took place at the relaxation stage. Angles γ and θ at the

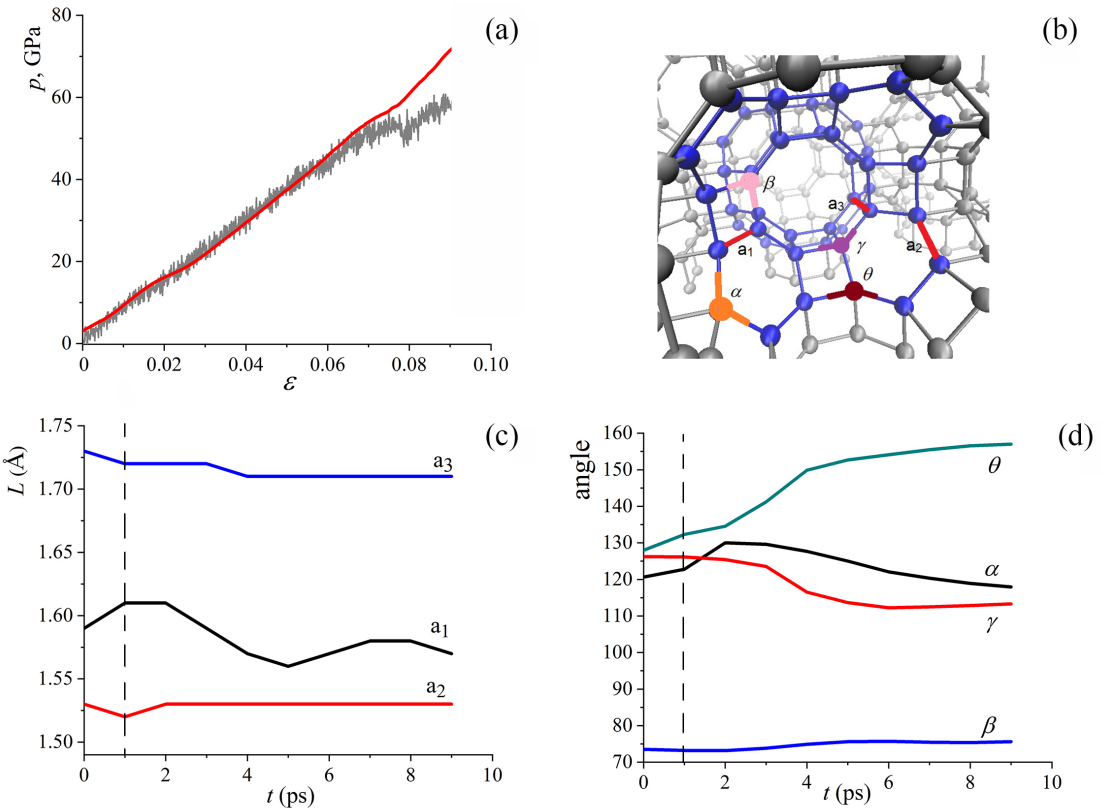

Figure 2. Phase CA7 at hydrostatic compression: (a) pressure-strain curves at T=1 K (red curve) and T=300 K (gray curve); (b) structural element with the analyzed angles and bonds; (c,d) change of the values of covalent bonds (c) and valent angles (d) in course of deformation at T=1 K.

initial state was equal to 135° and during relaxation change to about 128°, β change from 90° to 73°, α has not changed. Length of the lattice constants also changing: a_1 change to 6% (from 1.5 to 1.59 Å), a_2 - 2% (from 1.5 to 1.53 Å) and a_3 - 10% (from 1.57 to 1.73 Å).

During compression θ increases to 157° and γ decreases to 113°. These angles mostly contribute to the compression dynamics of CA7. Angles α changing from 120° to 118° and γ - from 126° to 113°. The bond lengths a_2, a_3 almost not changing, while a_1 significantly and non-monotonously changes during compression. At the final moment, the bonds are a_1=1.57 Å, a_2=1.53 Å, and a_3=1.71 Å. Analysis of the radial distribution function at different strain showed that fullerane CA7 transform into an amorphous state at about ε=0.07. At this value, a plateau in the pressure-strain curve also can be seen.

3.2. Tubulanes

Fig. 3a shows hydrostatic pressure as the function of strain for tubulane TA5. Diamond-like phase TA5 reaches a critical stress (p=62 GPa) at $\varepsilon =\sim 0.036$ as it can be seen from Fig. 3a. Temperature smooths the pressure-strain curves slightly, but again have no considerable effect on the compression process. From the analysis of changing of covalent bonds and valent angles, it can be seen that angles α and θ change reversely: α decreases and θ increases in comparison with the initial values. The angles β and γ change in the same way during relaxation.

During compression, all angles change slightly: α – from 104° to 102°, β – from 114° to 113°, γ – from 114° to 113° and θ – from 75° to 77°. The lengths of all bonds are reduced almost equally, by 2%: in initial moment $a_1 = 1.49$ Å, $a_2 = 1.6$ Åand $a_3 = 1.68$ Åand at the final moment of compression $a_1 = 1.42$ Å, $a_2 = 1.55$ Åand $a_3 = 1.66$ Å. As for fulleranes, tubulanes do not lose their crystalline order and do not become amorphous to high densities. Here, compression is occured mainly because of covalent bonds decrease with the small changes of valent angles.

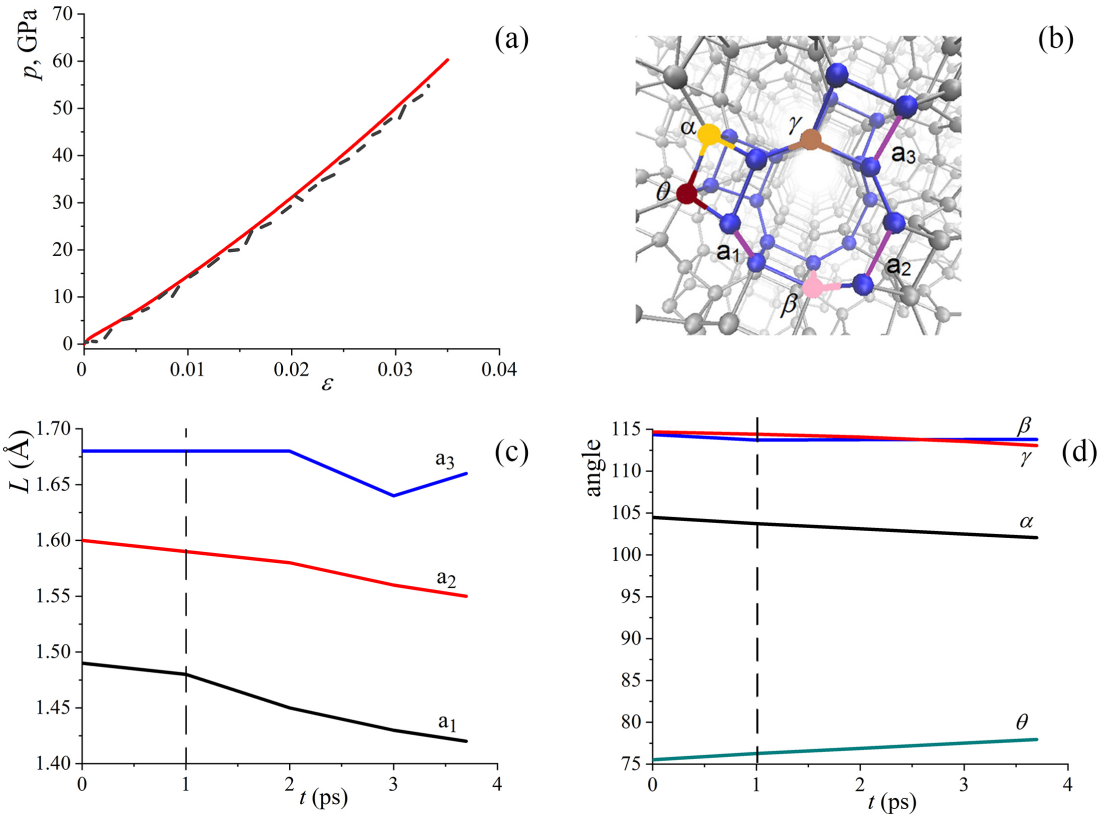

Figure 3. The same as in Fig. 2, but for TA5.

4. Conclusions

The molecular dynamics simulation is used to study the stability and deformation behavior of carbon diamond-like phases based on fullerene-like molecules and nanotubes. Stable configurations are identified, and the main mechanisms of phase deformation are found. In the field of elastic deformation, stiffness and compliance constants were calculated.

In common, DLPs of different morphology show similar behaviour and can be analysed on example of single phase. However, there are some differences which can be explained by special structural configurations. A numerical experiment showed that some stable DLPs can be hydrostatically compressed to densities close to the density of diamond. It was found that the phases are deformed in a similar way due to changes in bond lengths and angles depending on the morphological features of a particular phase. Hydrostatic compression occurs mainly because of the changes in the valent angles and bonds for all DLPs. However, some phases can

transform into the amorphous state which can be seen from the plateau on the pressure-strain curve and from the analysis of radial distribution function.

5. Acknowledgments

Calculation of the elastic constants was supported by the Grant of the President of the Russian Federation for state support of young Russian scientists - doctors of sciences MD-1651.2018.2. MD of deformation behaviour was supported by the State Assignment of IMS RAS.

6. References

[1] Kvashnin A G, Sorokin P B and Chernozatonskii L A 2018 *Comp. Mater. Sci.* **142** 32–37
[2] Savin A V, Korznikova E A and Dmitriev S V 2016 *Lett. Mater.* **6** 77–81
[3] Chernozatonskii L A and Demin V A 2018 *JETP Lett.* **107** 315–319
[4] Baimova J A and Rysaeva L K 2018 *Journal of Structural Chemistry* **59** 884–890
[5] Katin K P and Maslov M M 2018 *Molecular Simulation* **44** 703–707
[6] Savin A V and Mazo M A 2018 *2D Chain models of nanoribbon scrolls* (Springer International Publishing) chap Molecular dynamics of polymer crystals and nanostructures, pp 241–262
[7] Brazhkin V V and Solozhenko V L 2019 *J. Appl. Phys.* **125** 130901
[8] Belenkov E A and Shabiev F K 2015 *Letters on Materials* **5** 459–462
[9] Belenkov E A and Tingaev M I 2015 *Letters on Materials* **5** 15–19
[10] Zhao Z, Xu B, Wang L M, Zhou X F, He J, Liu Z, Wang H T and Tian Y 2011 *ACS Nano* **5** 7226–7234
[11] Flores-Livas J A, Lehtovaara L, Amsler M, Goedecker S, Pailhès S, Botti S, Miguel A S and Marques M A L 2012 *Phys. Rev. B* **85** 155428
[12] Hu M, Huang Q, Zhao Z, Xu B, Yu D and He J 2014 *Diamond Relat. Mater.* **46** 15–20
[13] Mujica A, Pickard C J and Needs R J 2015 *Phys. Rev. B* **91** 214104
[14] Kulnitskiy B, Perezhogin I, Dubitsky G and Blank V 2013 *Acta Cryst. B* **69** 474–479
[15] Öhrström L and O'Keeffe M 2013 *Z. Kristallogr. Cryst. Mater.* **228** 343–346
[16] Esser M, Esser A A, Proserpio D M, Dronskowski R 2017 *Carbon* **121** 154–162
[17] Krylova K A, Baimova Y A, Dmitriev S V and Mulyukov R R 2016 *Physics of the Solid State* **58** 394–401
[18] Bewilogua K and Hofmann D 2014 *Surface and Coatings Technology* **242** 214–225
[19] Greshnyakov V A, Belenkov E A, Berezin V M 2012 *Crystal structure and properties of diamond-like carbon phase* vol 150
[20] Belenkov E A and Greshnyakov V A 2016 *Physics of the Solid State* **58** 2145–2154
[21] Greshnyakov V and Belenkov E A 2016 *Materials Science Forum* **845** 231–234
[22] Greshnyakov V A and Belenkov E A 2018 *IOP Conference Series: Materials Science and Engineering* **447** 012018
[23] Belenkov E A and Greshnyakov V A 2018 *Physics of the Solid State* **60** 1294–1302
[24] Baimova J A, Rysaeva L Kh, Dmitriev S V, Lisovenko D S, Gorodtsov V A, Indeitsev D A 2017 *Materials Physics and Mechanics* **33** 1–11
[25] Lisovenko D S, Baimova Y A, Rysaeva L K, Gorodtsov V A and Dmitriev S V 2017 *Physics of the Solid State* **59** 820–828
[26] Rysaeva L K, Baimova J A, Dmitriev S V, Lisovenko D S, Gorodtsov V A and Rudskoy A I 2019 *Diamond Relat. Mater.* **97** 107411
[27] Lisovenko D S, Baimova J A, Rysaeva L K, Gorodtsov V A, Rudskoy A I and Dmitriev S V 2016 *Phys. Status Solidi B* **253** 1295–1302
[28] Mavrinskii V and Belenkov E 2018 *Letters on Materials* **8** 169–173
[29] Rysaeva L K 2017 *Journal of Physics: Conference Series* **938** 012071
[30] Goldstein R, Lisovenko D, Chentsov A and Lavrentyev S 2017 *Letters on Materials* **7** 355–358
[31] Goldstein R V, Gorodtsov V A and Lisovenko D S 2015 *Physical Mesomechanics* **18** 213–222
[32] Goldstein R V, Gorodtsov V A, Lisovenko D S and Volkov M A 2014 *Physical Mesomechanics* **17** 97–115
[33] Goldstein R V, Gorodtsov V A and Lisovenko D S 2013 *Letters on Materials* **3** 7–11